

## A Novel Conductance Measurement Technique for Profiling the Lateral LDD n-Doping Concentrations of Submicron MOS Devices

Steve S. Chung, G. H. Lee, S. M. Cheng, and M. S. Liang\*

Department of Electronic Engineering, National Chiao Tung University, Hsinchu, Taiwan, R.O.C.

\*Taiwan Semiconductor Manufacturing Co., Hsinchu Science-based Industrial Park., Hsinchu, Taiwan, R.O.C.

This paper reports a simple I-V method for the first time to determine the lateral lightly-doped source/drain (S/D) profiles ( $n^-$  region) of LDD n-MOSFETs. One interesting application is the direct observation of the reverse-short-channel effect (RSCE)<sup>1)</sup>. It is observed that S/D  $n^-$  doping profile is channel length dependent if reverse short channel effect exists as a result of the interstitial imperfections caused by OED(Oxide Enhanced Diffusion) or S/D implant. Not only the lateral profile of long channel devices but also the short channel devices can be determined. It is an indispensable tool for the device drain engineering work in the current ULSI technology.

### 1. Introduction

In the device drain engineering, not only the S/D vertical profile but also its lateral profile is rather important for the submicron device design. For the S/D vertical profile, it can be characterized by SIMS or SRP measurement. To determine the lateral profile, a few<sup>2-4)</sup> were reported based on the capacitance measurement method. However, all of these methods are for S/D  $n^+$  profile only. None has been developed so far to determine the lateral  $n^-$  doping profile.

Recently, a so called Reverse-Short-Channel Effect (RSCE), has aroused much interests. This effect is commonly attributed to a lateral nonuniform doping profile along the channel. Poly-gate reoxidation<sup>1)</sup>, source/drain implant damage<sup>5)</sup>, and salicidation<sup>6)</sup> in the submicron CMOS process have been identified as the cause for the above enhanced dopant diffusion. For the direct verification of the existing RSCE, various methods such as the decoupled C-V technique<sup>7)</sup>, the measured  $V_T$ -L curve<sup>1)</sup> conventional C-V method<sup>8)</sup>, and charge pumping method<sup>9)</sup> have been employed to show the existence of the non-uniform channel doping effects. In this work, we will for the first time propose a simple I-V method that allows direct determination of the lateral lightly-doped S/D ( $n^-$ ) profiles for MOSFETs. Then, appropriate modification is carried out to characterize the boron-redistribution-induced RSCE in short-channel devices. Furthermore, applications to justify the S/D profile in drain engineering (e.g., LATID devices) were made. Finally, to show the validity and applicability of this method, the results have also been justified by using 2D simulation.

### 2. Experimental

Devices used in this study were fabricated using a poly-Si gate 0.6 $\mu$ m CMOS technology. The spacer width is 0.25 $\mu$ m. The split conditions for S/D  $n^-$  implant are Phosphorous 80keV, ( $2 \times 10^{13}$  cm<sup>-2</sup>,  $4 \times 10^{13}$  cm<sup>-2</sup>) with 0°, 30°, 45° and 60° tilt angle implants. The channel implant is BF<sub>2</sub> ( $3.2 \times 10^{12}$  cm<sup>-2</sup>, 70keV).

The S/D  $n^+$  implant is As ( $3 \times 10^{15}$  cm<sup>-2</sup>, 80keV). All the devices have same drawn gate width 20 $\mu$ m but varying drawn gate lengths from 0.35 $\mu$ m to 20 $\mu$ m.

### 3. Paired I-V Method to Determine the Lateral S/D $n^-$ Doping Profile

It has been reasonably agreed that  $L_{eff}$  can be defined as the distance between the two points where the gate-induced carrier density  $Q_n$  (in cm<sup>-2</sup>) equals the doping profile  $N_{S/D,2D}$  (in cm<sup>-2</sup>) along the channel on S/D sides, as shown in Fig. 1. By applying the "paired  $V_{GS}$  method" as in<sup>10)</sup>,  $\Delta L$  and extrinsic  $R_{ext}$  as the functions of  $V_{GS}$  can be determined and shown in Figs. 2 and 3. Here,  $R_{tot}$  is the total source-to-drain resistance. The correlation between doping  $N_{S/D,2D}$  and  $Q_n$  can be expressed by eq. (1), where  $Q_n$  is the inversion carrier density at small  $V_{DS}$ . Also, by assuming the impurity doping profile being a Gaussian distribution with projected range  $\Delta R_p$ , as shown in Fig.4(a),  $N_{S/D,3D}$  can be related to  $N_{S/D,2D}$  by eq.(2). As a consequence, the S/D profiles along the channel can be directly determined by diagrammatic manipulation as shown in Fig. 4(b) using the equations listed in Table 1. Results of the extracted S/D profiles for two different  $n^-$  dosages are shown in Fig. 5. We can see that LDD devices with higher  $n^-$  dosage exhibit a heavier concentration moving toward the center of the channel, as expected.

### 4. Boron-redistribution Effect from the Characterized S/D Doping Profiles

By observing the results from the  $R_{tot}$ - $L_m$  curve shown in the inset of Fig.2, it can be seen that an anomalous behavior occurs, in which the values of  $R_{tot}$  deviate farther away from the fitting line due to the channel impurity nonuniformity as the device length shrinks. If we modify the previously-described method to determine  $\Delta L$  and  $R_{ext}$  for short- and long-channel devices respectively, it will be shown that both the extracted  $\Delta L$  and  $R_{ext}$  for long-channel devices (denoted by  $\Delta L_l$  and  $R_{ext,l}$ ) are larger than those for short-channel devices (denoted by  $\Delta L_s$  and  $R_{ext,s}$ ), while those (denoted

by  $\Delta L_{all}$  and  $R_{ext,all}$  fitted in the full channel length range (from  $.5\mu\text{m}$  to  $20\mu\text{m}$ ) give results much closer to  $\Delta L_I (R_{ext,I})$  compared to  $\Delta L_S (R_{ext,S})$ , as demonstrated in Fig. 6. It means that as long as RSCE exists in short-channel devices, the extracted values are different from those of long-channel devices. Fig. 7 shows the corresponding  $n^-$  profiles from  $\Delta L_S$  and  $\Delta L_I$  versus  $V_G$  respectively. The  $n^-$  profile for short-channel devices moves back towards the outside of the active channel region, and also becomes more lightly-doped than that for long-channel devices. As noted earlier, this redistribution is a result of the nonuniformity in the channel doping profile as illustrated schematically in Fig. 8. In other words, the nonuniformity  $\Delta N_B(x)$  in the channel profile (boron), that results in RSCE, will cause the moving of  $n^-$  profile boundaries for short- and long-channel devices. As shown in Fig. 6, this method can also provide the capability for direct investigation into the existence of RSCE from the comparison between  $\Delta L_S$  and  $\Delta L_I$  curves. If there is no RSCE existing in short-channel devices, these two curves should coincide together. In contrast, if RSCE becomes more significant, these two curves will deviate farther away from each other. Fig. 9 shows the simulated net doping profile along the channel for devices with and without OED<sup>1)</sup> by SUPREM IV. It confirms the movement of the net profile as a result of boron redistribution.

## 5. Further Applications of the Present Method

For another practical application in the device drain engineering, S/D  $n^-$  profiles for the other LATID devices are also extracted and for a comparison in Fig. 10, in which larger tilt angle  $n^-$  implant has higher value of lateral doping and moves deeper into the channel. The lateral diffusion length ( $L_{n^-}$ ) from the spacer edge to the drain junction can also be determined as given in Fig. 11 which provides important information for device drain engineering work.

In summary, by using the conductance measurement technique in this paper, for the first time our studies show that: (1) the lateral doping profile (along the channel) of the lightly-doped  $n^-$  S/D region in LDD devices can be directly calculated, (2) the RSCE as a result of the process or channel implant-induced effect for the tested devices can be qualitatively and quantitatively determined, (3) the present method can be used as a monitor of the nonuniform lateral channel doping distribution in the state-of-the-art submicron VLSI/ULSI CMOS process and device design, and (4) it provides us an efficient tool for device drain engineering studies.

**Acknowledgements** This work was sponsored by the National Science Council under contract NSC83-0404-E009-101 and in part by the Tsmc, Hsinchu Science-based Industrial Park, Taiwan.

## References

- 1) M. Orlowski *et al.*, in *IEDM Tech. Dig.*, p. 632, 1987.
- 2) J. Scarpulla *et al.*, in *IEDM Tech. Dig.*, p.722, 1987.
- 3) W. Rosner *et al.*, in *Dig. of Symp. on VLSI Tech.*, p. 9, 1988.

- 4) H. Uchida *et al.*, in *Dig. of Symp. on VLSI Tech.*, p. 39, 1993.
- 5) T. kunikiyo *et al.*, in *NUPAD IV Tech. Dig.*, P. 51, 1992.
- 6) C. Y. Lu *et al.*, *IEEE EDL*, vol. EDL-10, p. 446, 1989.
- 7) J. Guo *et al.*, *Japan J. Appl. Phys.*, p. 630, 1994.
- 8) C. Y. Chang *et al.*, *IEEE EDL*, vol. 15, p. 437, 1994.
- 9) S. S. Chung *et al.*, in *Symp. VLSI Tech. Dig.*, p. 103, 1995.
- 10) G. Hu *et al.*, *IEEE Trans. ED.*, vol. ED-33, p. 2469, 1987.

$$Q_n(V_{GS}) = \frac{C_{ox}}{q} (V_{GS} - V_{Th} - 0.5V_{DS}) = N_{S/D,2D} \quad (1)$$

$$N_{S/D,2D} = 2\sqrt{\Sigma\Delta R_p} N_{S/D,3D} \quad (2)$$

$$N_{S/D,3D} = k \cdot (V_{GS} - V_{Th} - 0.5V_{DS}) \quad (3)$$

where

$$k = \frac{C_{ox}}{2\sqrt{\Sigma\Delta R_p} q}$$

$$R_{ext} = R_{sp} + R_n \cdot + R_n \cdot + R_{co} \approx R_{sp} + R_n \cdot \quad (4)$$

Table 1 Equations for deriving the doping concentration from inversion layer charge density.

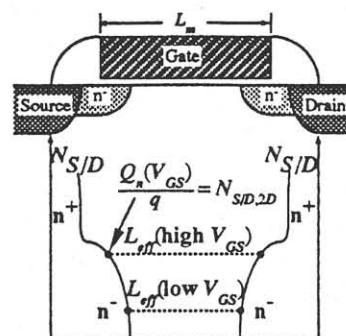


Fig. 1 A schematic carrier density plot along the channel and the definition of  $L_{n^-}$  at low or high gate biases.

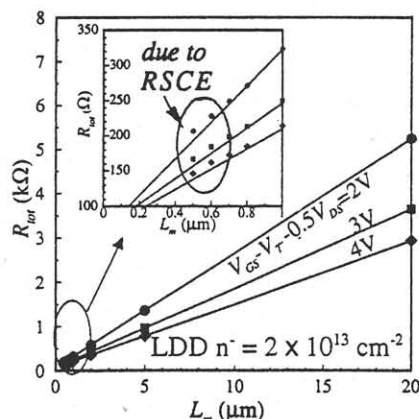


Fig. 2 Measured  $R_{10}/L_m$  for LDD n-MOSFET's with  $n^- = 2 \times 10^{13} \text{cm}^{-2}$ . Deviation of the measured data for short channel devices from the fitted line shows the observed RSCE.

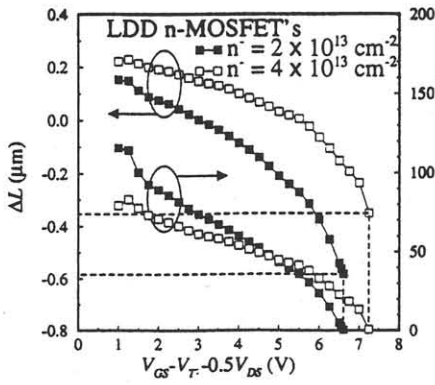


Fig. 3 Extracted  $\Delta L$  and  $R_{ext}$  versus gate drive ( $V_{GS} - V_T - 0.5V_{DS}$ ) from long channel devices for two different  $n^-$  dosages.

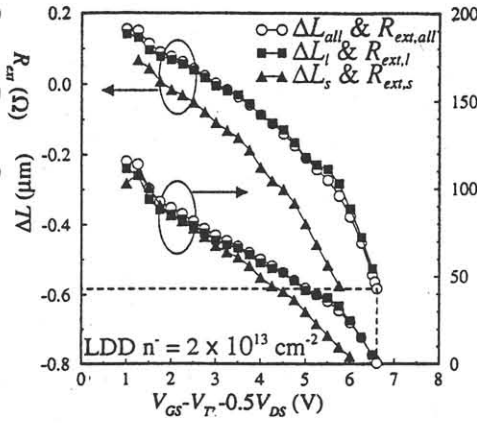


Fig. 6  $\Delta L$  and  $R_{ext}$  vs. ( $V_{GS} - V_T - 0.5V_{DS}$ ) extracted for short-channel ( $L_m = 0.5\mu m$ ) and long-channel ( $L_m = 20\mu m$ ) devices.

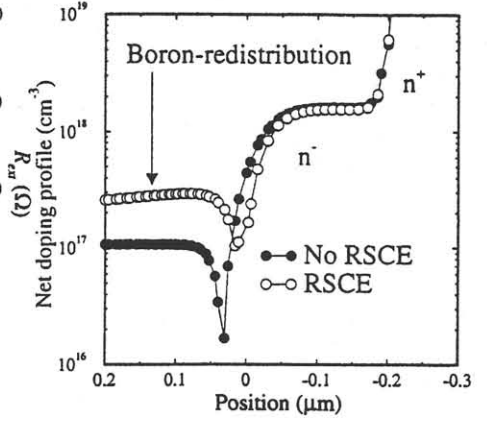


Fig. 9 The change in the net doping profile simulated by SUPREM IV for devices with and without OED. Due to RSCE, the  $n^-$  profile moves back towards the outside of the active channel region.

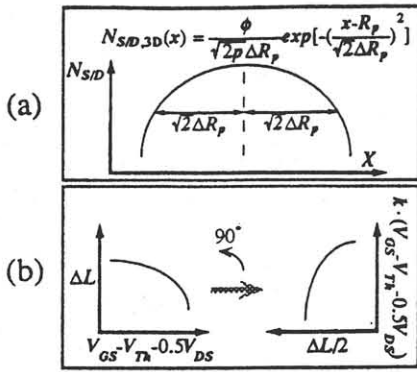


Fig. 4 Schematic illustration of the transformation from the  $\Delta L$  versus gate drive into doping distribution along the channel.

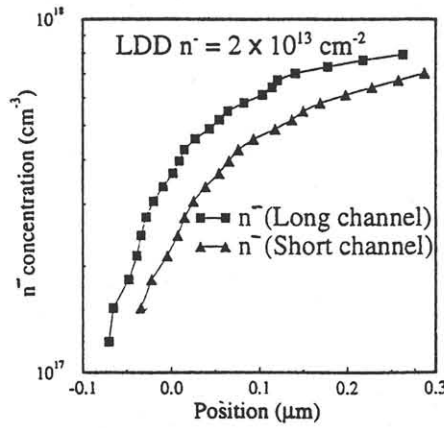


Fig. 7 Extracted lateral  $n^-$  profiles for LDD MOSFET's with  $n^- = 2 \times 10^{13} \text{ cm}^{-2}$  for short-channel and long-channel devices.

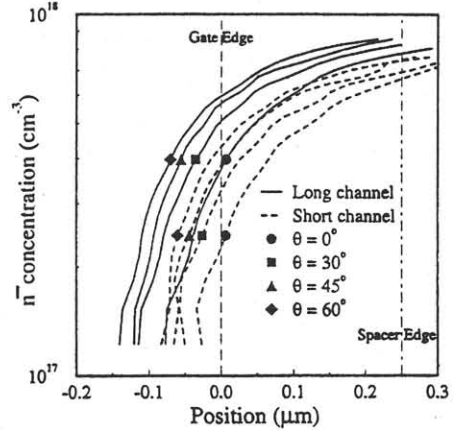


Fig. 10 Extracted lateral S/D doping profiles for LATID devices with  $n^- = 2 \times 10^{13} \text{ cm}^{-2}$ .

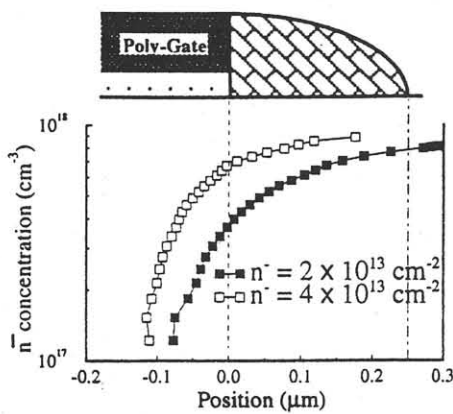


Fig. 5 Extracted lateral S/D  $n^-$  profiles for a long channel device  $L_m = 20\mu m$  with different  $n^-$  dosages from Fig. 3.

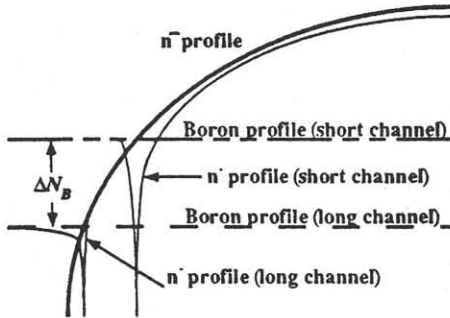


Fig. 8 Qualitative description of the variations in channel doping profile due to RSCE.  $\Delta N_B$  is the boron redistribution effect.

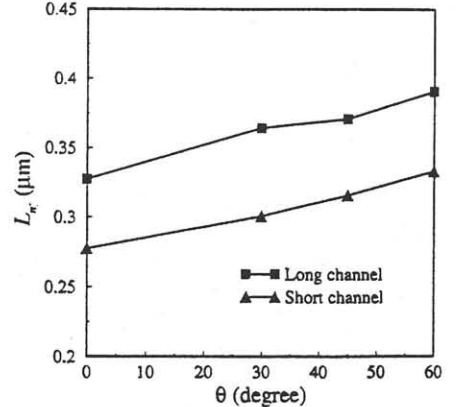


Fig. 11 Extracted  $L_n$  (spacer edge to the S/D junction) for various LATID devices.